crystals

MDPI

Article

X-ray Structures and Hirshfeld Studies of Two Dinuclear Cd(II) Complexes with a *s*-Triazine/Pyrazolo Ligand and Pesudohalides as a Linker

Saied M. Soliman [1,*], Hessa H. Al-Rasheed [2,*], Sarah A. AL-khamis [2], Matti Haukka [3] and Ayman El-Faham [1]

[1] Department of Chemistry, Faculty of Science, Alexandria University, P.O. Box 426, Ibrahimia, Alexandria 21321, Egypt; ayman.elfaham@alexu.edu.eg
[2] Department of Chemistry, College of Science, King Saud University, P.O. Box 2455, Riyadh 11451, Saudi Arabia; 441203438@student.ksu.edu.sa
[3] Department of Chemistry, University of Jyväskylä, P.O. Box 35, FI-40014 Jyväskylä, Finland; matti.o.haukka@jyu.fi
* Correspondence: saeed.soliman@alexu.edu.eg (S.M.S.); halbahli@ksu.edu.sa (H.H.A.-R.); Tel.: +20-111-136-1059 (S.M.S.)

Abstract: The two dinuclear Cd(II) complexes $[Cd(BPMST)(SCN)]_2$ (**1**) and $[Cd(BPMST)(N_3)Cl]_2$ (**2**) of a *s*-triazine/pyrazolo ligand (**BPMST**) were synthesized. The preparation of both complexes was performed in a water–ethanol solvent mixture and involved the mixing of the functional ligand **BPMST** with $CdCl_2$ in the presence of thiocyanate or azide as linkers, respectively. The dinuclear formula of both complexes and the involvement of the pesudohalide as a linker between the Cd(II) centers were approved by single crystal X-ray structures. The Cd(II) was hexa-coordinated and the CdN_5S (**1**) and CdN_5Cl (**2**) coordination environments had distorted octahedral geometry. In the $[Cd(BPMST)(SCN)]_2$ and $[Cd(BPMST)(N_3)Cl]_2$, the **BPMST** acted as a pincer tridentate N-chelate. In the case of **1**, the SCN^- acted as a *μ(1,3)* bridging ligand between the Cd(II) centers, while the N_3^- had a *μ(1,1)* bridging mode in **2**. As a result, the Cd. . .Cd distance was significantly longer in **1** (5.8033(5) Å) than in **2** (3.796(2) Å). In both complexes, the Cd(II) had distorted octahedral coordination geometry. Hirshfeld surface analysis was performed to inspect the supramolecular aspects of the two Cd(II) complexes. The C. . .H, N. . .H and S. . .H contacts were important in the case of $[Cd(BPMST)(SCN)]_2$ (**1**). Their percentages were calculated to be 14.7, 17.0 and 13.4%, respectively. In the case of $[Cd(BPMST)(N_3)Cl]_2$ (**2**), the most significant contacts were the Cl. . .H, C. . .H and N. . .H contacts. Their contributions in the molecular packing were 16.5, 9.7 and 25.3%, respectively. The propensity of atom pairs of elements to form contacts in the crystal structure was analyzed using enrichment ratio (E_{XY}).

Keywords: cadmium; *s*-triazine; X-ray structure; supramolecular; Hirshfeld; d_{norm}

check for updates

Citation: Soliman, S.M.; Al-Rasheed, H.H.; AL-khamis, S.A.; Haukka, M.; El-Faham, A. X-ray Structures and Hirshfeld Studies of Two Dinuclear Cd(II) Complexes with a *s*-Triazine/Pyrazolo Ligand and Pesudohalides as a Linker. *Crystals* **2023**, *13*, 1198. https://doi.org/10.3390/cryst13081198

Academic Editor: Vladimir P. Fedin

Received: 20 July 2023
Revised: 29 July 2023
Accepted: 31 July 2023
Published: 2 August 2023

Copyright: © 2023 by the authors. Licensee MDPI, Basel, Switzerland. This article is an open access article distributed under the terms and conditions of the Creative Commons Attribution (CC BY) license (https://creativecommons.org/licenses/by/4.0/).

1. Introduction

Cadmium is an extremely poisonous heavy metal [1–4]. Despite this well-known fact, Cd and its compounds are of great importance. Cd serves as a catalytic center in carbonic anhydrase [5]. Also, it has interesting DNA binding abilities [6–8], antibacterial activities [9,10] and antitumor properties [11,12] and is a known catalyst for organic transformations [13–18]. Also, Cd(II) compounds have many applications in photoluminescence and non-linear optics [19–22]. Cd(II) coordination compounds with N-donor ligands have successful applications in ligand exchange chromatography [23–25]. Also, Cd(II) complexes have interesting and versatile applications in nanoscience [26,27]. From an electronics point of view, Cd(II) has high flexibility to form complexes with diverse coordination numbers ranging from four to eight. In this regard, the self-assembly method is a very simple technique used for the synthesis of coordination compounds with fascinating molecular and supramolecular structures [28–37].

s-triazines are attractive ligands for researchers interested in building interesting coordination compounds due to their flexible coordination behavior [38–43] and brilliant ability to construct metal complexes with fascinating supramolecular structures [44–46]. *s*-triazine coordination compounds are stable compounds with fascinating properties [47–55]. In addition, the highly symmetric structure of *s*-triazine (*s*-Trz) moiety is an important requirement in crystal engineering for the construction of interesting supramolecular structures [56–66]. *s*-triazine derivatives with two pyrazolyl (Pyz) arms (Figure 1) are considered tridentate chelates capable of binding metal ions in a pincer mode, leading to fascinating and stable metal complexes [45,67–73].

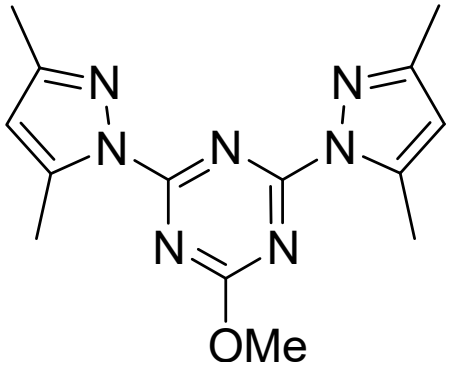


Figure 1. Structure of the **BPMST**.

2,4-*Bis*(3,5-dimethyl-1H-pyrazol-1-yl)-6-diethylamino-1,3,5-triazine is a structurally related pincer ligand analog for the **BPMST** ligand. The crystal structures of the pesudohalide complexes of 2,4-*bis*(3,5-dimethyl-1H-pyrazol-1-yl)-6-diethylamino -1,3,5-triazine with the d^7–d^{10} metal ion were reported. It was found that the Co(II) and Cu(II) metal ions formed mononuclear pesudohalide complexes. In the case of Ni(II), dinuclear pesudohalide complexes were obtained. The surface photovoltage (SPV) response suggested these complexes to extend to semiconductor materials [67]. Recently, a number of mononuclear complexes of the **BPMST** ligand were presented by our research group [45,68–74]. In order to increase the nuclearity of the complex, a linker such as azide or thiocyanate could be used to achieve this target. In this work, the reaction products of the self-assembly of $CdCl_2$ with **BPMST** in the presence of azide or thiocyanate as linkers were presented. Their X-ray structures were presented for the first time. In addition, their supramolecular structures were investigated using Hirshfeld analysis.

2. Materials and Methods

All details for chemicals and solvents are mentioned in the Supplementary Data.

2.1. Syntheses

The ligand BPMST was prepared according to the described method by our research team [44,45].

Synthesis of the Cd(II) Complexes[Cd(BPMST)(SCN)]$_2$ (**1**) and [Cd(BPMST)(N_3)Cl]$_2$ (**2**)

A total of 10 mL of **BPMST** (0.06 g, 0.2 mmol) in EtOH was mixed with $CdCl_2$ (0.037 g, 0.2 mmol) in 5 mL of distilled H_2O in the presence of 0.5 mL of a saturated aqueous KSCN or NaN_3 solution. The complexes [Cd(BPMST)(SCN)]$_2$ (**1**) and [Cd(BPMST)(N_3)Cl]$_2$ (**2**) were assembled from the solution as colorless crystals after 8 and 10 days, respectively.

The yields were as follows: $C_{16}H_{17}CdN_9OS_2$ (**1**): 89.1%. Anal. Calc. N, 23.88; H, 3.25; C, 36.4; Cd, 21.29%. Found: N, 23.67; H, 3.16; C, 36.14; Cd, 21.11%. IR (KBr, cm^{-1}): 3103, 2137, 2033, 1606, 1541; Figure S1 (Supplementary Data). $C_{14}H_{17}CdClN_{10}O$ (**2**): 82.1%. Anal. Calc. N, 28.63; H, 3.50; C, 34.37; Cd, 22.98. Found: N, 28.40; H, 3.39; C, 34.05; Cd, 22.77%. FTIR (KBr, cm^{-1}): 3115, 3022, 2959, 2048, 1596, 1572, 1538; Figure S2 (Supplementary Data).

2.2. Crystal Structure Determination

The single crystal structure of complexes **1** and **2** was determined using a Bruker D8 Quest diffractometer. The experimental details are provided in Method S1 (Supplementary Data) [75]. Crystal data are depicted in Table S1.

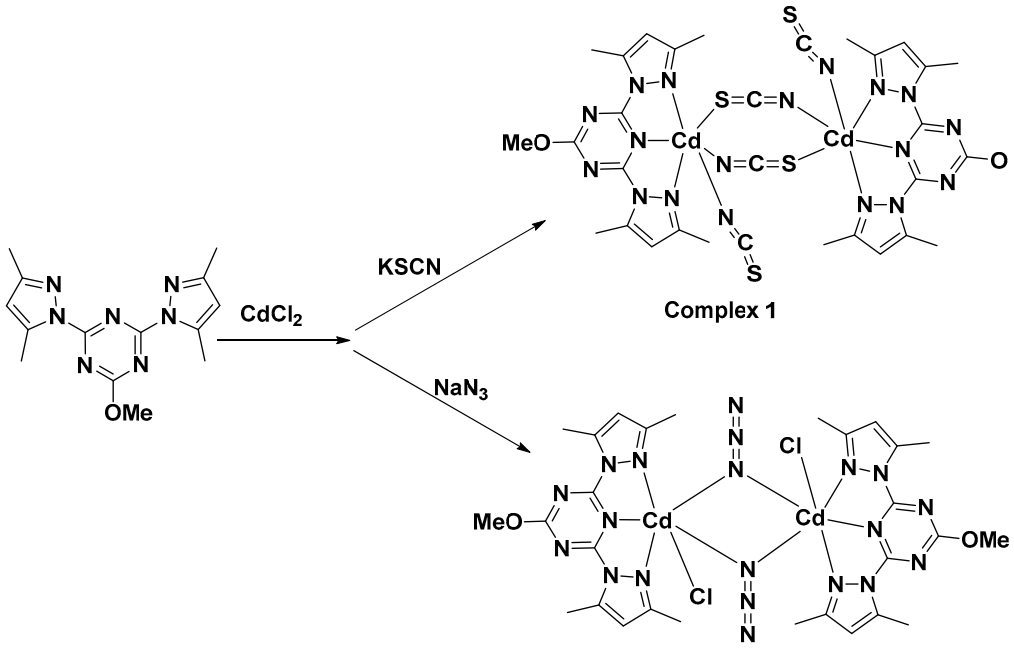
2.3. Hirshfeld Surface Analysis

The Crystal Explorer [76] program was used to generate the 2D fingerprint plots and study the Hirshfeld surfaces.

3. Results and Discussion

3.1. Synthesis and Characterizations

In previous studies, the pincer ligand, 2,4-bis(3,5-dimethyl-1H-pyrazol-1-yl)-6-diethyla mino-1,3,5-triazine, gave mononuclear pseudohalide complexes with Cu(II) and Co(II) ions. On the other hand, the dinuclear pesudohalide complexes that are not commonly reported in the literature on this class of ligand were obtained in the case of Ni(II) [74]. In the current study, the two dinuclear Cd(II) complexes, $[Cd(BPMST)(SCN)]_2$ (**1**) and $[Cd(BPMST)(N_3)Cl]_2$ (**2**), were synthesized by mixing equimolar amounts of **BPMST** with $CdCl_2$ in the presence of thiocyanate or azide as a linker in a water–ethanol solvent mixture. The two products were isolated in a highly crystalline form and in good yields. Solving the structure with the aid of single-crystal X-ray diffraction confirmed the dinuclear formula of the Cd(II) complexes and the involvement of the pesudohalide as a linker connecting the two Cd(II) ions (Scheme 1). In addition, FTIR spectra showed two sharp bands characteristic of the bridged SCN^- at 2137 and 2033 cm^{-1} in the case of complex **1**. The sharp band at 2048 cm^{-1} in the FTIR spectra of complex **2** confirmed the presence of the bridged azide. In the FTIR spectra of complexes **1** and **2**, the vibrational characteristics of the **BPMST** were detected with some variation compared to those of the free **BPMST**. While the $\upsilon_{C=C}$ and $\upsilon_{C=N}$ modes of the free **BPMST** were observed at 1555 and 1593 cm^{-1}, respectively (), the corresponding values in the case of complex **1** were detected at 1606 and 1541 cm^{-1}, respectively. For **2**, the $\upsilon_{C=N}$ modes were detected as a doubly split band at 1596 and 1572 cm^{-1}, while the $\upsilon_{C=C}$ mode was detected at 1538 cm^{-1} (Figures S1–S3, Supplementary Data).



Scheme 1. Synthesis of complexes $[Cd(BPMST)(SCN)]_2$ (**1**) and $[Cd(BPMST)(N_3)Cl]_2$ (**2**).

3.2. Crystal Structure Description

The X-ray structure of the $[Cd(BPMST)(SCN)]_2$ complex is shown in Figure 2. The results indicated a dinuclear structure in which there is one [Cd(BPMST)(SCN)] as an asymmetric formula where two of these units were connected by the bridged *μ(1,3)* thiocyanate groups. The complex crystallized in the orthorhombic crystal system and space group *Pbca* with the unit cell parameters were determined to be a = 14.6614(5) Å, b = 15.9147(6) Å and c = 18.0194(7) Å. The unit cell volume was 4204.5(3) $Å^3$ and the calculated crystal density was 1.668 g/cm^3.

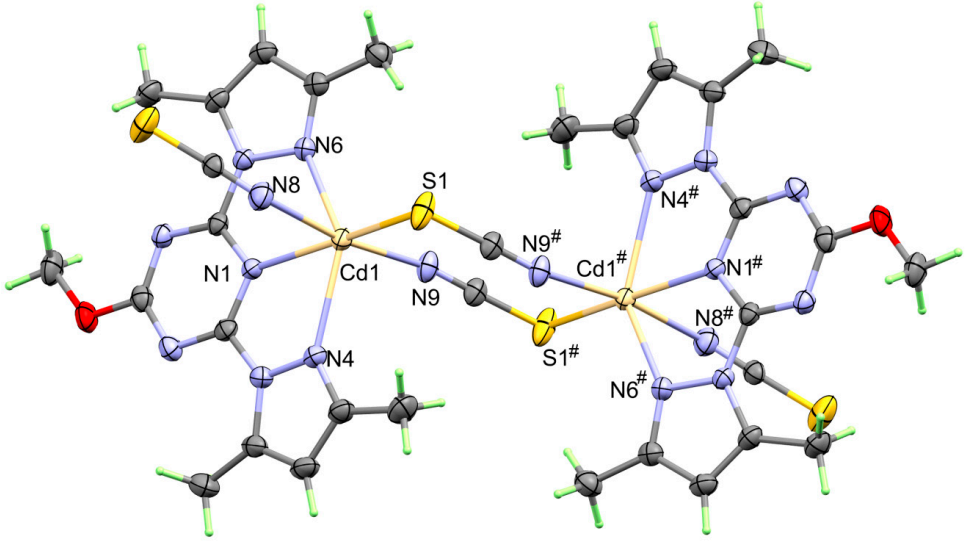


Figure 2. X-ray structure of $[Cd(BPMST)(SCN)]_2$ complex (**1**). Symmetry code #: 1 − x, 1 − y, −z.

In this dinuclear complex, the Cd(II) had a CdN_5S hexa-coordination environment. There were three short Cd1-N4 (2.402(3) Å), Cd1-N6 (2.454(3) Å) and Cd1-N1 (2.348(3) Å) bonds with the **BPMST** ligand. Hence, the **BPMST** ligand acted as tridentate N-chelate via two N-atoms (N4 and N6) from the Pyz moieties and another N-atom (N1) from the *s*-Trz core. The bite angles N6-Cd1-N1 (66.06(9)°) and N1-Cd1-N4 (66.63(10)°) of the **BPMST** ligand were almost the same, while the trans-N4-Cd1-N6 was almost twice this value (131.93(10)°). In addition, the Cd(II) was coordinated with three SCN^- groups. Two of the SCN^- groups were bridged ligands connecting the two crystallographically dependent Cd(II) centers via Cd1-N9 (2.6170(11) Å) and Cd1-S1 (2.258(3) Å) bonds where the N9-Cd1-S1 angle was 92.07(8)°. The third SCN^- group was terminal and coordinated with the Cd(II) center via N8, where the respective Cd1-N8 bond distance was 2.287(3) Å, which was shorter than the corresponding Cd1-N9 bond of the bridged thiocyanate. The trans N9-Cd1-N8 angle was 171.72(12)°, while the cis S1-Cd1-N8 angle was 84.40(9)°. Details of the geometric parameters for the coordination sphere are listed in Table 1. It was clear that the CdN_5S coordination sphere had a distorted octahedral configuration. Due to the *μ(1,3)* bridging mode of the thiocyanate group, the distance between the crystallographically related Cd sites was quite large. The Cd1. . .Cd1 distance was determined to be 5.8033(5) Å.

The supramolecular structure of the $[Cd(BPMST)(SCN)]_2$ complex was dominated by a weak C12-H12A. . .N8 interaction. The acceptor N8 to donor C12 distance was 3.454(4) Å, while the hydrogen H12A to acceptor N8 distance was 2.660 Å. Views of the C12-H12A. . .N8 contacts and packing scheme are shown in Figures 3 and 4, respectively.

Table 1. Bond lengths (Å) and angles (°) for the $[Cd(BPMST)(SCN)]_2$ complex (**1**).

Bond	Length/Å	Bond	Length/Å
Bond distances			
Cd1-N9 #	2.258(3)	Cd1-N4	2.402(3)
Cd1-N8	2.287(3)	Cd1-N6	2.454(3)
Cd1-N1	2.348(3)	Cd1-S1	2.6170(11)
Bond angles			
N9 #-Cd1-N8	171.72(12)	N1-Cd1-N6	66.06(9)
N9 #-Cd1-N1	99.30(10)	N4-Cd1-N6	131.93(10)
N8-Cd1-N1	84.99(11)	N9 #-Cd1-S1	92.07(8)
N9 #-Cd1-N4	87.14(11)	N8-Cd1-S1	84.40(9)
N8-Cd1-N4	101.09(12)	N1-Cd1-S1	167.45(7)
N1-Cd1-N4	66.63(10)	N4-Cd1-S1	108.99(8)
N9 #-Cd1-N6	92.31(11)	N6-Cd1-S1	119.06(7)
N8-Cd1-N6	82.93(12)		

1 − x, 1 − y, −z.

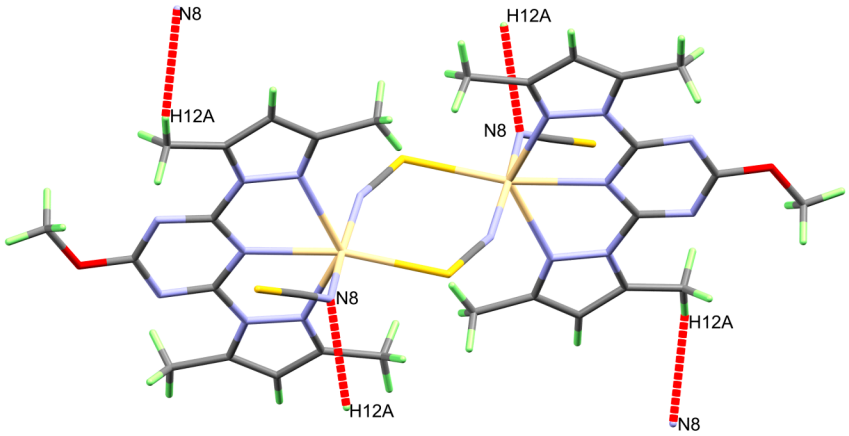


Figure 3. The N. . .H intermolecular contacts in the $[Cd(BPMST)(SCN)]_2$ complex (**1**).

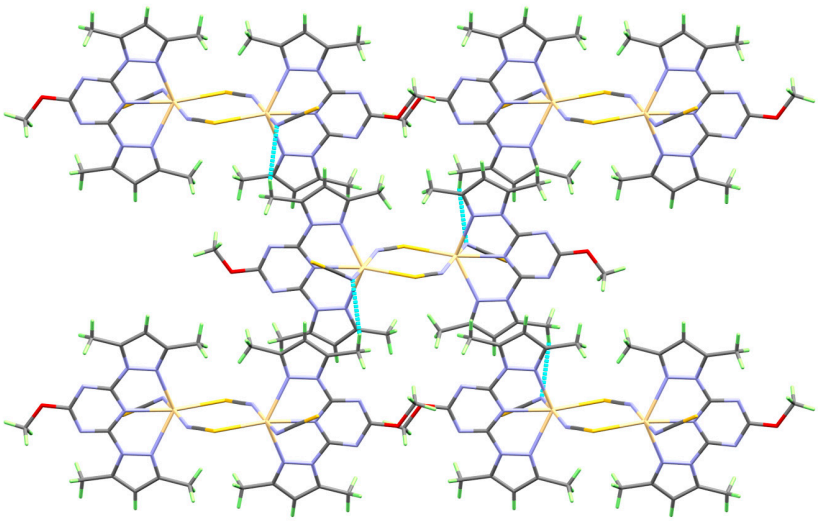


Figure 4. Packing structure for the $[Cd(BPMST)(SCN)]_2$ complex (**1**).

In addition, the terminal thiocyanate group with the free S2 atom that did not participate in a coordination interaction with the Cd(II) ion was involved in anion-π stacking interactions with the coordinated *s*-triazine group. The S2. . .C3 contact distance was 3.497(3) Å and a presentation for this anion-π stacking interaction is shown in Figure 5.

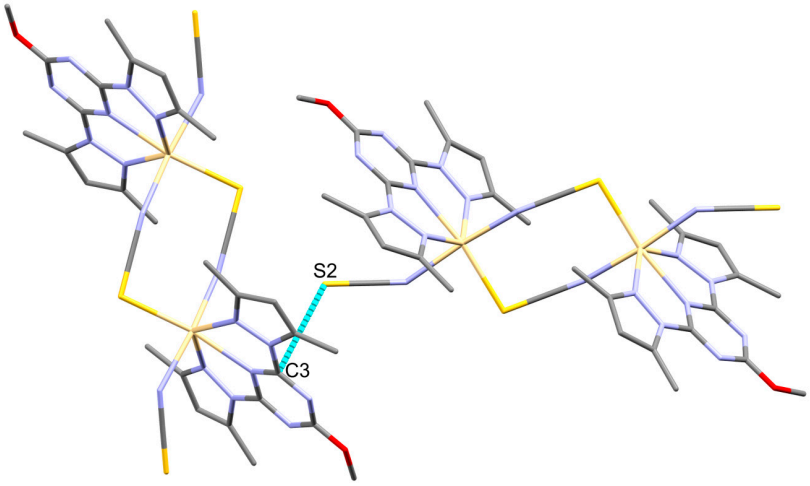


Figure 5. The anion-π stacking interactions in the $[Cd(BPMST)(SCN)]_2$ complex (**1**).

The structure analysis for the single crystal of the $[Cd(BPMST)(N_3)Cl]_2$ complex is depicted in Table S1. The formula $[Cd(BPMST)(N_3)Cl]$ represents the asymmetric unit of the dinuclear complex. The two $[Cd(BPMST)(N_3)Cl]$ units were connected by the bridged azide groups. In this case, the crystal system was triclinic and the space group was *P-1*. The triclinic crystal parameters were a = 9.323(4) Å, b = 10.936(5) Å, c = 11.312(5) Å, α = 112.637(10)°, β = 104.547(11)° and γ = 105.133(10)°. The unit cell volume was 944.2(12) $Å^3$ and the calculated crystal density was 1.721 g/cm^3. The structure of the $[Cd(BPMST)(N_3)Cl]_2$ complex is shown in Figure 6.

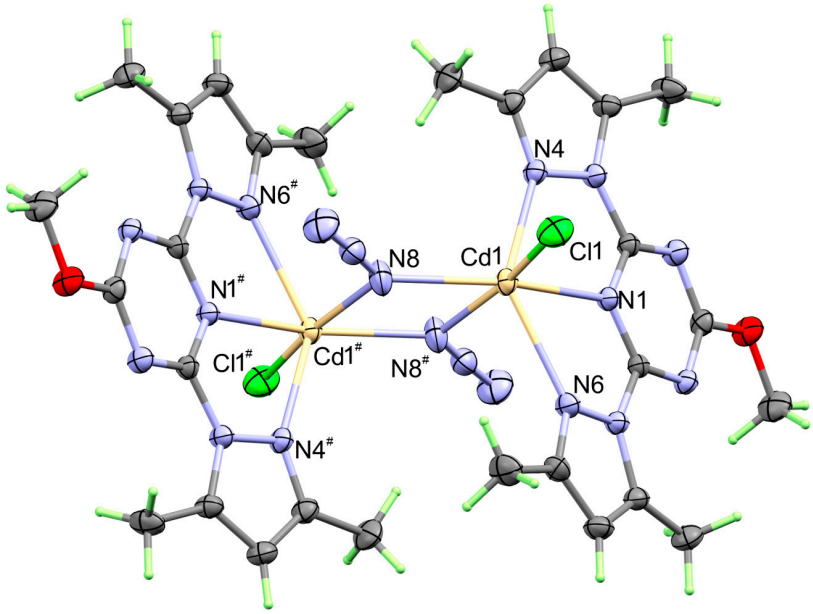


Figure 6. X-ray structure of $[Cd(BPMST)(N_3)Cl]_2$ (**2**). Symmetry code #: 1 − x, 2 − y, 1 − z.

The structure of the dinuclear azido complex $[Cd(BPMST)(N_3)Cl]_2$ was quite different. In this case, the Cd(II) ion was coordinated to one **BPMST** ligand unit also as a tridentate pincer ligand. The Cd1-N1, Cd1-N4 and Cd1-N6 distances were determined to be 2.411(2), 2.409(2) and 2.451(2) Å, respectively. In this case, the distance between the Cd1 site and the N1-atom of the *s*-triazine core was not the shortest, while the Cd1-N4 with one of the pyrazolyl moieties was the shortest. Also, the bite angles N1-Cd1-N6 (64.57(7)°) and N1-Cd1-N4 (65.64(7)°) of the **BPMST** ligand were almost the same, but both were slightly less than those found in the $[Cd(BPMST)(SCN)]_2$ complex. The trans-N4-Cd1-N6 was 130.14(7)°, which was also twice the bite angle values. The coordination sphere of the

Cd(II) was accomplished by two *μ(1,1)* bridged azide ions and one terminal chloride ion (Figure 6). The Cd1-N8 and Cd1-N8# distances were determined to be 2.415(3) and 2.322(3) Å, respectively. In this case, the distance between the crystallographically related Cd sites was significantly small (3.796(2) Å) compared to the corresponding Cd…Cd distance in the $[Cd(BPMST)(SCN)]_2$ complex. The Cd1-Cl1 distance was 2.4700(13) Å, and a list of the angles around the coordination environment is depicted in Table 2. It is clear that all bond angle values deviated significantly from the ideal values of the perfect octahedron. Hence, the CdN_5Cl coordination sphere had a distorted octahedral configuration.

Table 2. Bond lengths (Å) and angles (°) for the $[Cd(BPMST)(N_3)Cl]_2$ complex (**2**).

Bond	Length/Å	Bond	Length/Å
Bond distances			
Cd1-Cl1	2.4700(13)	Cd1-N8 #	2.322(3)
Cd1-N4	2.409(2)	Cd1-N1	2.411(2)
Cd1-N8	2.415(3)	Cd1-N6	2.451(2)
Bond angles			
N8 #-Cd1-N4	109.11(10)	N8 #-Cd1-N1	154.32(9)
N4-Cd1-N1	65.64(7)	N8-Cd1-N8 #	73.49(12)
N4-Cd1-N8	90.55(10)	N1-Cd1-N8	81.31(8)
N8 #-Cd1-N6	116.69(10)	N4-Cd1-N6	130.14(7)
N1-Cd1-N6	64.57(7)	N8-Cd1-N6	84.58(10)
N8 #-Cd1-Cl1	95.60(8)	N4-Cd1-Cl1	95.94(6)
N1-Cd1-Cl1	109.80(6)	N8-Cd1-Cl1	168.70(7)
N6-Cd1-Cl1	98.15(7)		

1 − x, 1 − y, −z.

The packing of the $[Cd(BPMST)(N_3)Cl]_2$ complex was controlled by a weak C12-H12C…N10 interaction. The donor C12 to acceptor N10 distance was 3.547(6) Å, while the hydrogen H12C to acceptor N10 distance was 2.61 Å. Views of the C12-H12C…N10 contacts and packing scheme are shown in Figure 7.

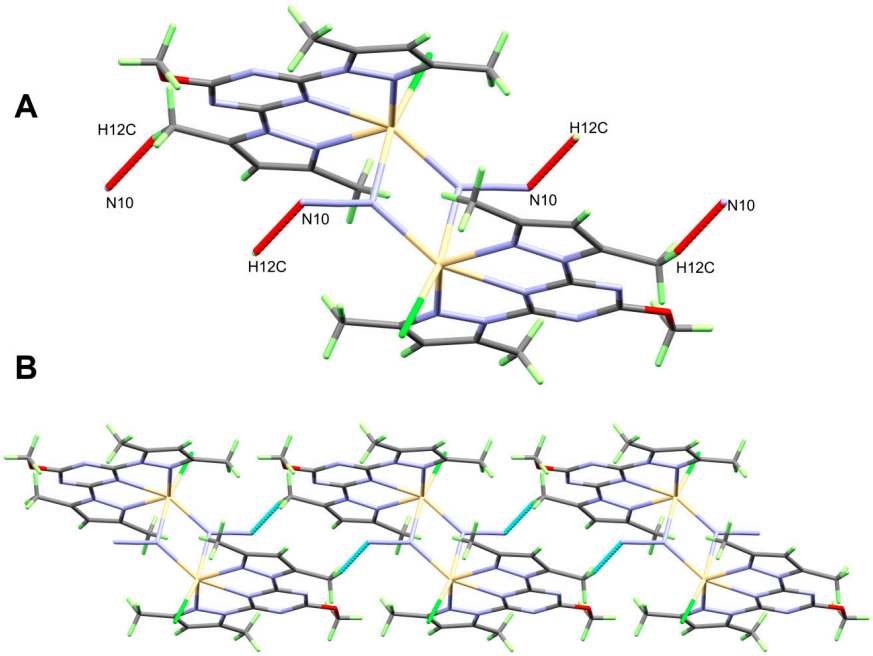


Figure 7. The N…H intermolecular interactions (**A**) and packing view (**B**) for the $[Cd(BPMST)(N_3)Cl]_2$ complex (**2**).

In addition, the $[Cd(BPMST)(N_3)Cl]_2$ units were connected by some Cl. . .H interactions between the coordinated chloride ion as an H-bond acceptor with C14-H14A as an H-bond donor (Figure 8). The acceptor Cl1 to donor C14 distance was 3.638(4) Å.

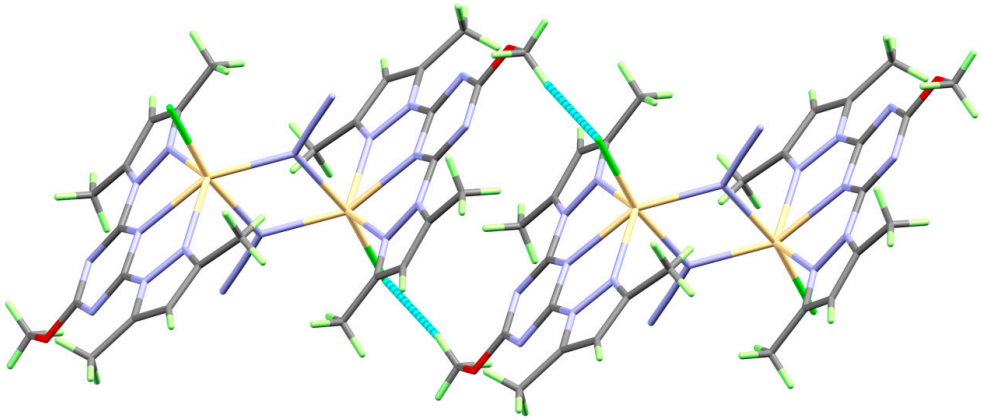


Figure 8. The packing structure of the $[Cd(BPMST)(N_3)Cl]_2$ complex via Cl. . .H intermolecular contacts.

3.3. Analysis of Molecular Packing

The crystalline materials were characterized by a well-organized arrangement, which kept the crystal stable via a complicated set of non-covalent interactions involving hydrogen bonds, C-H. . .π, anion-π interactions, etc. Hirshfeld topology analysis is a lead method for detecting all possible non-covalent interactions that control the stability of a crystal structure. The different Hirshfeld surfaces for the complex $[Cd(BPMST)(SCN)]_2$(**1**) are shown in Figure 9. It is clear that the d_{norm} map showed some red spots. These red spots are related to regions involved in short non-covalent interactions with neighboring molecules. The most important non-covalent interactions were the C. . .H, N. . .H and S. . .H contacts, which are labeled as **A**, **B** and **C**, respectively. C14. . .H16C, N8. . .H12A and S2. . .H5 were the shortest interactions, where the corresponding contact distances were 2.627, 2.567 and 2.881 Å, respectively.

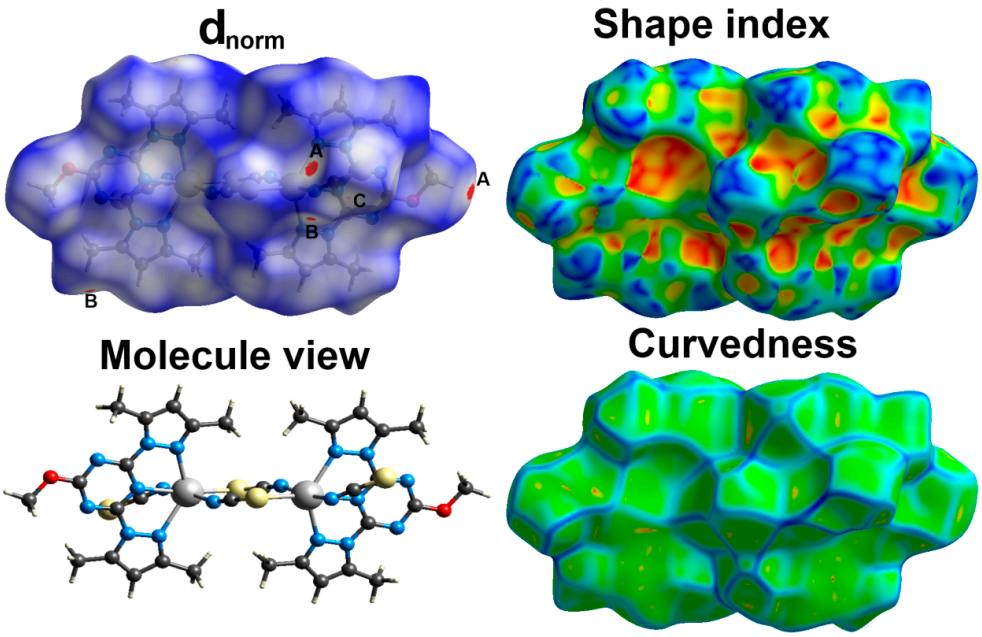


Figure 9. Hirshfeld surfaces for $[Cd(BPMST)(SCN)]_2$ (**1**). **A**, **B** and **C** are related to C. . .H, N. . .H and S. . .H interactions, respectively.

In addition, Figure 10 shows the characteristic fingerprint plots of the C. . .H, N. . .H and S. . .H interactions. The appearance of these contacts as spikes in the corresponding fingerprint plots indicated their relevance in the molecular packing of the $[Cd(BPMST)(SCN)]_2$ complex. In addition, the area of the colored region of each plot gave an indication of the percentages of these intermolecular contacts. The percentages of the C. . .H, N. . .H and S. . .H interactions were calculated to be 14.7, 17.0 and 13.4%, respectively.

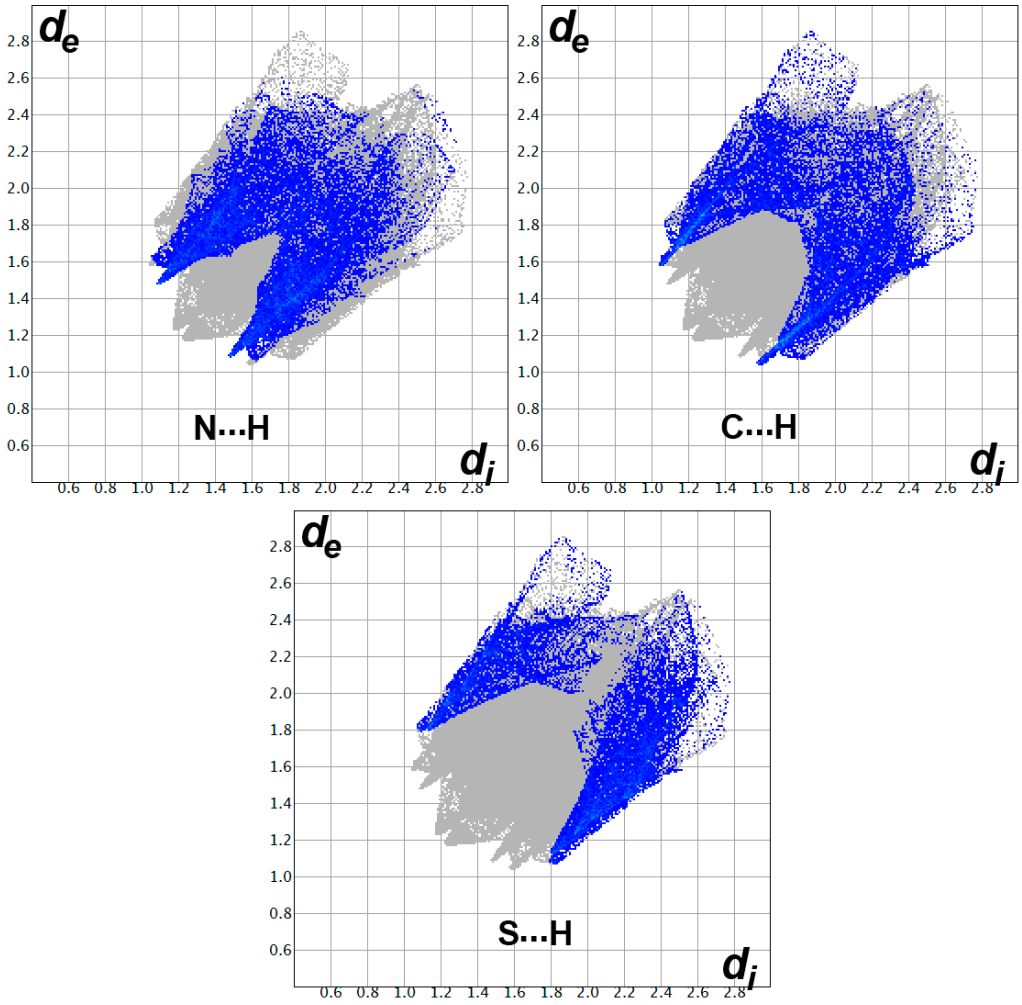


Figure 10. Fingerprint plots for the C. . .H, N. . .H and S. . .H interactions in the complex $[Cd(BPMST)(SCN)]_2$ (**1**).

In addition, there were many other weak interactions that affected the supramolecular structure of the $[Cd(BPMST)(SCN)]_2$ complex. A summary of all interactions and their contributions to the molecular packing are shown in Figure 11. The most common interaction was hydrogenic H. . .H contacts (35.7%). In addition, there was a small number of weak S. . .C contacts that contributed 3.4% of all interactions. This interaction appears as a white region in the d_{norm} map, indicating equal interaction distance to the vdWs radii sum of the S and C atoms. Hence, the anion-π interaction in this complex was considered relatively weak.

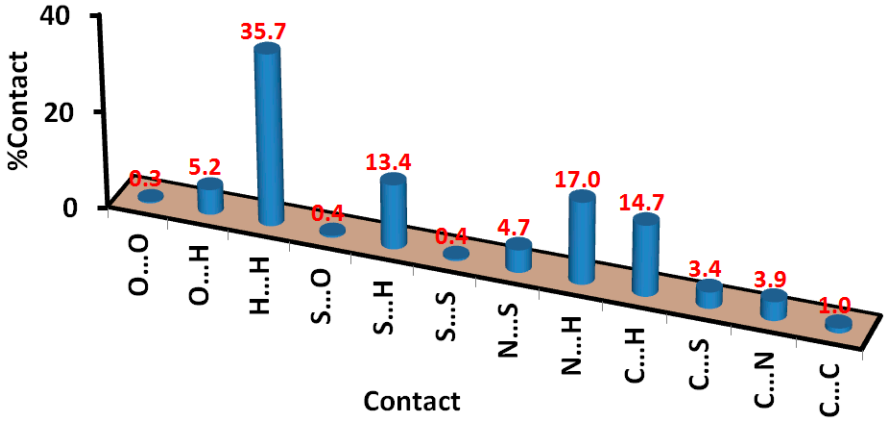


Figure 11. Intermolecular interactions in $[Cd(BPMST)(SCN)]_2$ (**1**).

For the $[Cd(BPMST)(N_3)Cl]_2$ complex (**2**), the different Hirshfeld maps are presented in Figure 12. In this case, the red spots in the d_{norm} map correspond to the Cl. . .H, C. . .H, N. . .H and H. . .H interactions. These contacts are labeled as letters **A** to **D**, respectively. Cl1. . .H14A, N10. . .H12C, C5. . .H11B and H13A. . .H13C were the shortest interactions. Their respective contact distances were 2.770, 2.485, 2.657 and 2.515 Å, respectively. Similar to the observation detected in the fingerprint plots of the $[Cd(BPMST)(SCN)]_2$ complex, the decomposed fingerprint plots of Cl. . .H, C. . .H and N. . .H appeared as sharp spikes (Figure 13). This was considered further evidence of the significance of these interactions in the molecular packing of the $[Cd(BPMST)(N_3)Cl]_2$ complex (**2**).

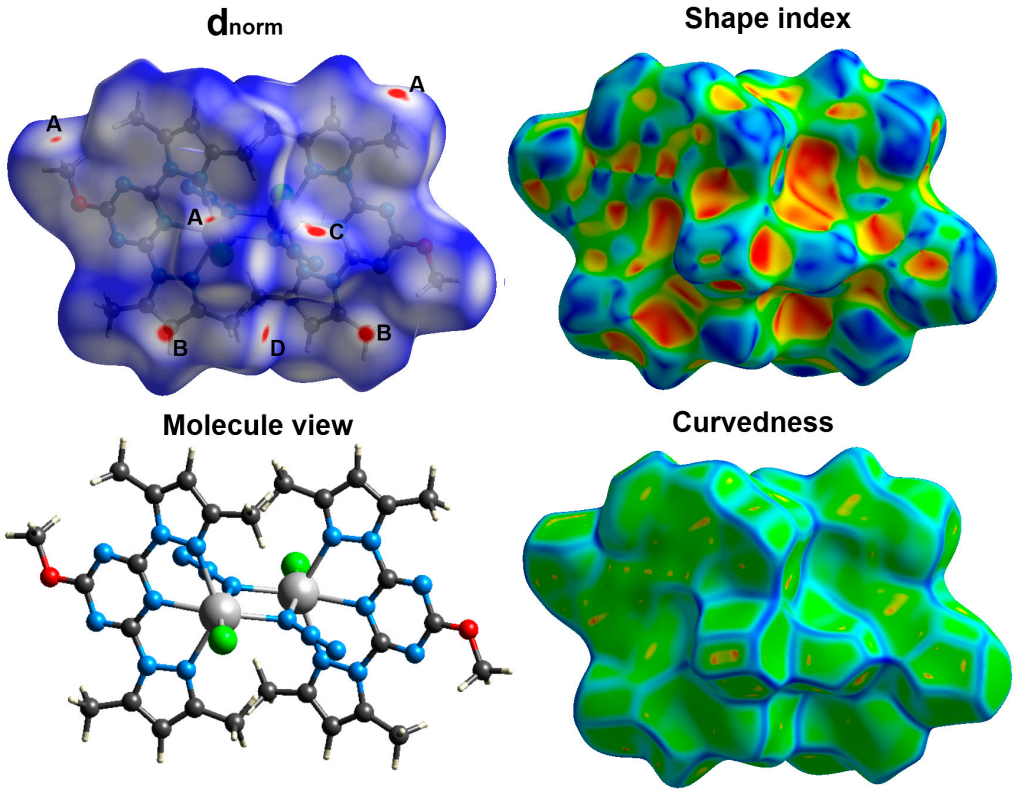


Figure 12. Hirshfeld surfaces for the $[Cd(BPMST)(N_3)Cl]_2$ complex (**2**). The Cl. . .H (**A**), C. . .H (**B**), N. . .H (**C**) and H. . .H (**D**) contacts are shown in the d_{norm} map for clarity.

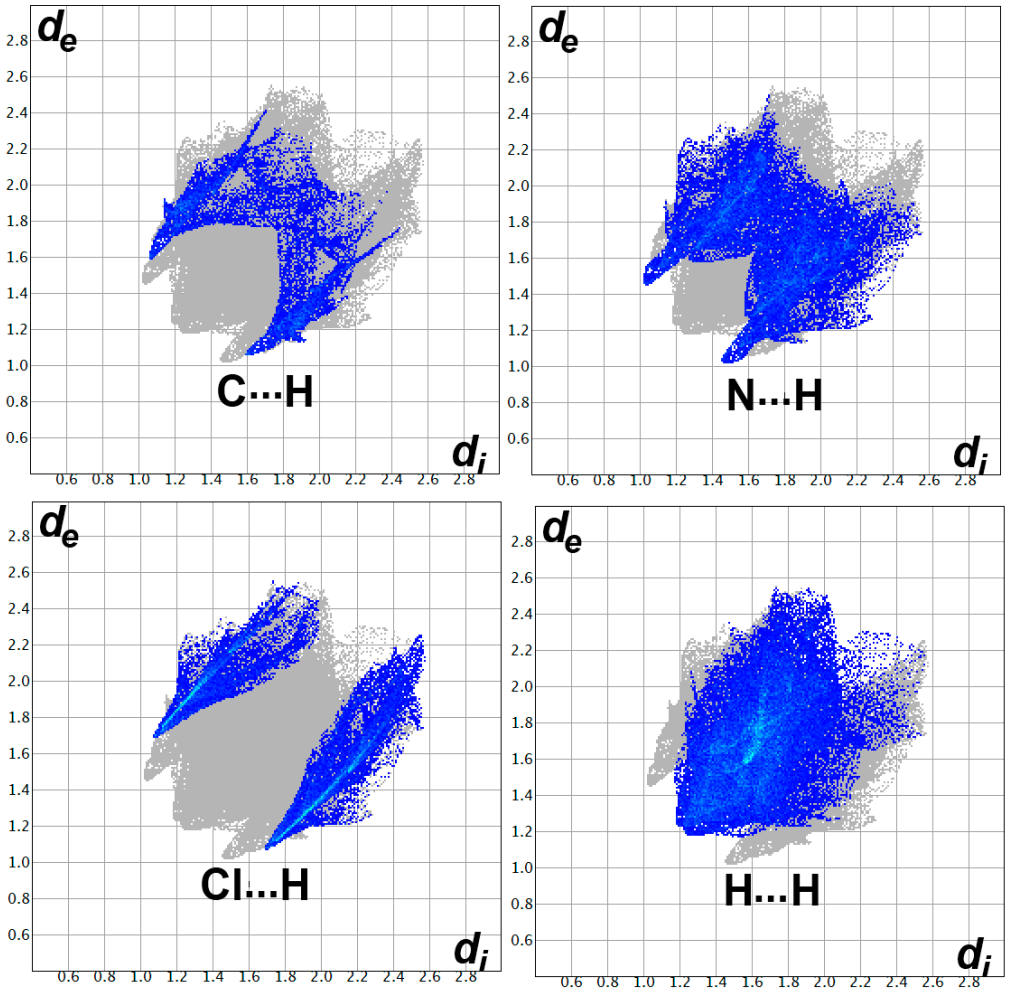


Figure 13. Fingerprint plots for the Cl…H, C…H, N…H and H…H interactions in the $[Cd(BPMST)(N_3)Cl]_2$ complex (**2**).

Additionally, the percentages of all possible non-covalent interactions that occurred in the $[Cd(BPMST)(N_3)Cl]_2$ complex (**2**) are shown in Figure 14. The percentages of the Cl…H, C…H, N…H and H…H contacts were 16.5, 9.7, 25.3 and 37.1%, respectively. In addition, there was a small contribution from the polar O…H interaction (6.4%), which appeared to be weak and had less important molecular packing compared to the Cl…H, C…H and N…H interactions.

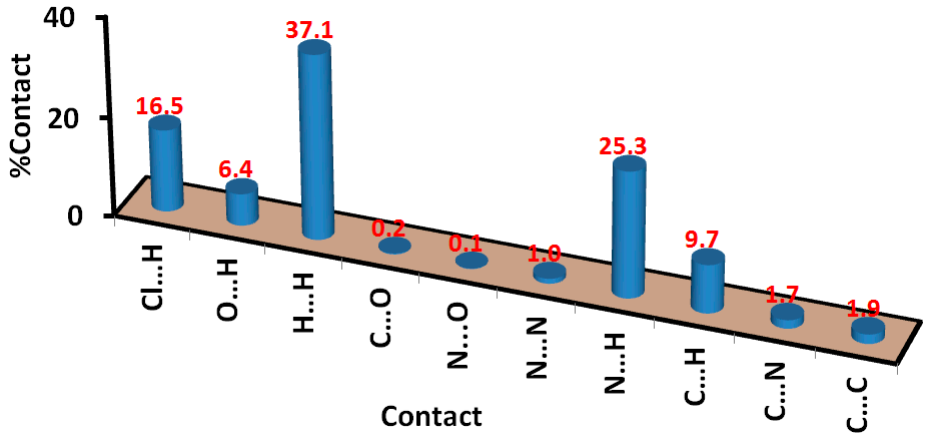


Figure 14. Intermolecular interactions in the $[Cd(BPMST)(N_3)Cl]_2$ complex (**2**).

In addition, the intermolecular interactions were further analyzed based on the enrichment ratio (E_{XY}) parameter [77]. The enrichment ratio (E_{XY}) of a pair of elements (X,Y) gave an indication of their propensity to form contacts in crystals. It is defined by the ratio of the proportion of the contact (C_{XY}) to the theoretical proportion of random contact (R_{XY}) [77]. The enrichment ratio is greater than 1 for atom pairs with a high propensity to form contacts. In contrast, the atom pairs that avoid contacts have an enrichment ratio lower than 1. The enrichment ratio E_{XY} of complexes **1** and **2** was calculated and the results are depicted in Table 3. In the case of the azido complex **2**, the enrichment ratio was greater than that for the Cl. . .H, O. . .H and N. . .H contacts and equal to one for the C. . .H interaction. On the other hand, $E_{XY} > 1$ for the O. . .H, N. . .H, N. . .S, C. . .N and C. . .S contacts, while $E_{XY} = 1$ for the C. . .H, S. . .H and H. . .H interactions. These results indicate that the atom pairs had a high propensity to form contacts. In contrast, the rest of the intermolecular contacts listed in the table showed a lower propensity to form contacts in the crystal structure.

Table 3. Enrichment ratio E_{XY} of the different inter-contacts in complexes $[Cd(BPMST)(SCN)]_2$ (**1**) and $[Cd(BPMST)(N_3)Cl]_2$ (**2**).

Enrichment Ratio (E_{XY})			
$[Cd(BPMST)(SCN)]_2$ (1)		**$[Cd(BPMST)(N_3)Cl]_2$ (2)**	
O. . .H	1.4	O. . .H	1.4
H. . .H	1.0	H. . .H	0.8
N. . .H	1.1	N. . .H	1.3
C. . .H	1.0	C. . .H	1.0
S. . .S	0.3	N. . .O	0.1
N. . .S	1.6	N. . .N	0.5
C. . .N	1.3	C. . .N	0.8
C. . .S	1.2	Cl. . .H	1.5
C. . .C	0.7		
S. . .H	1.0		

4. Conclusions

The self-assembly of the functional ligand **BPMST** with $CdCl_2$ in the presence of a linker such as thiocyanate or azide in a water–ethanol solution gave the dinuclear Cd(II) complexes $[Cd(BPMST)(SCN)]_2$ (**1**) and $[Cd(BPMST)(N_3)Cl]_2$ (**2**), respectively. The *s*-triazine/pyrazolo ligand (**BPMST**) acted as a pincer tridentate N-chelator. The pesudo-halides SCN^- and N_3^- acted as linkers between the two Cd(II) centers in *μ(1,3)* and *μ(1,1)* bridging modes, respectively. Analysis of the non-covalent interactions with the aid of Hirshfeld topology calculations indicated the importance of the C. . .H (14.7%), N. . .H (17.0) and S. . .H (13.4%) contacts in the molecular packaging of $[Cd(BPMST)(SCN)]_2$ (**1**). On the other hand, the Cl. . .H (16.5%), C. . .H (9.7%) and N. . .H (25.3%) interactions were the most significant in the supramolecular structure of $[Cd(BPMST)(N_3)Cl]_2$ (**2**). Enrichment ratio (E_{XY}) calculations were used to inspect the propensity of atom pairs of elements (X,Y) to form contacts in crystals.

Supplementary Materials: The following supporting information can be downloaded at https://www.mdpi.com/article/10.3390/cryst13081198/s1: Method S1 Crystal structure determination; Figure S1 FTIR spectra of **1**. Figure S2 FTIR spectra of **2;** Figure S3 FTIR spectra of **BPMST;** Table S1 Crystal data for complexes $[Cd(BPMST)(SCN)]_2$ (**1**) and $[Cd(BPMST)(N_3)Cl]_2$ (**2**).

Author Contributions: Conceptualization, S.M.S. and A.E.-F.; methodology, S.M.S. and M.H.; software, H.H.A.-R. and M.H.; validation, H.H.A.-R., S.A.A.-k. and S.M.S.; formal analysis, S.M.S. and H.H.A.-R.; investigation, S.M.S. and S.A.A.-k.; resources, A.E.-F. and H.H.A.-R.; data curation, S.M.S. and M.H.; writing—original draft preparation, S.M.S., H.H.A.-R., S.A.A.-k., M.H. and A.E.-F.; writing—review and editing, S.M.S., H.H.A.-R., S.A.A.-k., M.H. and A.E.-F.; visualization, S.M.S. and M.H.; supervision, S.M.S. and A.E.-F.; project administration, S.M.S., A.E.-F. and H.H.A.-R.; funding acquisition, H.H.A.-R. All authors have read and agreed to the published version of the manuscript.

Funding: The Deputyship for Research and Innovation, "Ministry of Education", King Saud University (IFKSUOR3-188-2), Saudi Arabia.

Data Availability Statement: All data generated or analyzed during this study are included in this published article.

Acknowledgments: The authors extend their appreciation to the Deputyship for Research and Innovation, "Ministry of Education" in Saudi Arabia for funding this research (IFKSUOR3-188-2).

Conflicts of Interest: The authors declare no conflict of interest.

References

1. Shibutani, M.; Mitsumori, K.; Niho, N.; Satoh, S.; Hiratsuka, H.; Satoh, M.; Sumiyoshi, M.; Nishijima, M.; Katsuki, Y.; Suzuki, J.; et al. Assessment of renal toxicity by analysis of regeneration of tubular epithelium in rats given low-dose cadmium chloride or cadmium-polluted rice for 22 months. *Arch. Toxicol.* **2000**, *74*, 571–577. [CrossRef]
2. Chen, L.; Lei, L.; Jin, T.; Nordberg, M.; Nordberg, G.F. Plasma Metallothionein Antibody, Urinary Cadmium, and Renal Dysfunction in a Chinese Type 2 Diabetic Population. *Diabetes Care* **2006**, *29*, 2682–2687. [CrossRef]
3. Antonio, M.T.; Corredor, L.; Leret, M.L. Study of the activity of several brain enzymes like markers of the neurotoxicity induced by perinatal exposure to lead and/or cadmium. *Toxicol. Lett.* **2003**, *143*, 331–340. [CrossRef] [PubMed]
4. Rikans, L.E.; Yamano, T. Mechanisms of cadmium-mediated acute hepatotoxicity. *J. Biochem. Mol. Toxicol.* **2000**, *14*, 110–117. [CrossRef]
5. Lane, T.W.; Morel, F.M.M. A biological function for cadmium in marine diatoms. *Proc. Natl. Acad. Sci. USA* **2000**, *97*, 4627–4631. [CrossRef]
6. Zhang, Z.Y.; Bi, C.F.; Fan, Y.H.; Yan, X.C.; Zhang, X.; Zhang, P.F.; Huang, G.M. Synthesis, crystal structures, luminescent properties, theoretical calculation, and DNA interaction of the cadmium (II) and lead (II) complexes with o-aminobenzoic acid and 1, 10-phenanthroline. *Russ. J. Coord. Chem.* **2015**, *41*, 274–284. [CrossRef]
7. Jana, S.K.; Mandal, A.K.; Seth, S.K.; Puschmann, H.; Hossain, M.; Dalai, S. Synthesis, Characterization and Crystal Structure of a New 3D Cadmium(II) Coordination Polymer: Binding Interaction with DNA and Double Stranded RNA. *J. Inorg. Organomet. Polym.* **2016**, *26*, 806–818. [CrossRef]
8. Zianna, A.; Ristović, M.Š.; Psomas, G.; Hatzidimitriou, A.; Coutouli-Argyropoulou, E.; Lalia-Kantouri, M. Cadmium(II) complexes of 5-bromo-salicylaldehyde and α-diimines: Synthesis, structure and interaction with calf-thymus DNA and albumins. *Polyhedron* **2016**, *107*, 136–147. [CrossRef]
9. Wazeer, M.I.M.; Isab, A.A.; Fettouhi, M. New cadmium chloride complexes with imidazolidine-2-thione and its derivatives: X-ray structures, solid state and solution NMR and antimicrobial activity studies. *Polyhedron* **2007**, *26*, 1725–1730. [CrossRef]
10. Ruíz, M.; Perelló, L.; Server-Carrió, J.; Ortiz, R.; García-Granda, S.; Díaz, M.R.; Cantón, E. Cinoxacin complexes with divalent metal ions. Spectroscopic characterization. Crystal structure of a new dinuclear Cd(II) complex having two chelate-bridging carboxylate groups. Antibacterial studies. *J. Inorg. Biochem.* **1998**, *69*, 231–239. [CrossRef]
11. Dubler, E.; Gyr, E. New metal complexes of the antitumor drug 6-mercaptopurine. Syntheses and X-ray structural characterizations of dichloro(6-mercaptopurinium)copper(I), dichlorotetrakis(6-mercaptopurine)cadmium(II), and bis(6-mercaptopurinato)cadmium(II) dehydrate. *Inorg. Chem.* **1988**, *27*, 1466–1473. [CrossRef]
12. Perez, J.M.; Cerrillo, V.; Matesanz, A.I.; Millan, J.M.; Navaro, P.; Alonso, C.; Souza, P. DNA Interstrand Cross-Linking Efficiency and Cytotoxic Activity of Novel Cadmium(II)–Thiocarbodiazone Complexes. *ChemBioChem* **2001**, *2*, 119–123. [CrossRef] [PubMed]
13. Ignatius, I.C.; Rajathi, S.; Kirubavathi, K.; Selvaraju, K. Synthesis, crystal growth and characterization of novel semiorganic nonlinear optical crystal: Dichloro(beta-alanine)cadmium(II). *Optik-Int. J. Light Electron. Opt.* **2014**, *125*, 5144–5147. [CrossRef]
14. Saghatforoush, L.; Khoshtarkib, Z.; Keypour, H.; Hakimi, M. Mononuclear, tetranuclear and polymeric cadmium(II) complexes with the 3,6-bis(2-pyridyl)-1,2,4,5-tetrazine ligand: Synthesis, crystal structure, spectroscopic and DFT studies. *Polyhedron* **2016**, *119*, 160–174. [CrossRef]
15. Wang, W.; Qiao, J.; Wang, L.; Duan, L.; Zhang, D.; Yang, W.; Qiu, Y. Synthesis, Structures, and Optical Properties of Cadmium Iodide/Phenethylamine Hybrid Materials with Controlled Structures and Emissions. *Inorg. Chem.* **2007**, *46*, 10252–10260. [CrossRef]
16. Biswas, F.B.; Roy, T.G.; Rahman, A.; Emran, T.B. An in vitro antibacterial and antifungal effects of cadmium (II) complexes of hexamethyltetraazacyclotetradecadiene and isomers of its saturated analogue. *Asian. Pac. J. Trop. Med.* **2014**, *7*, S534–S539. [CrossRef]
17. Yi, X.C.; Huang, M.X.; Qi, Y.; Gao, E.Q. Synthesis, structure, luminescence and catalytic properties of cadmium(II) coordination polymers with 9H-carbazole-2,7-dicarboxylic acid. *Dalton Trans.* **2014**, *43*, 3691–3697. [CrossRef]
18. Jia, W.G.; Li, D.D.; Gu, C.; Dai, Y.C.; Zhou, Y.H.; Yuan, G.; Sheng, E.H. Two cadmium(II) complexes with oxazoline-based ligands as effective catalysts for C–N cross-coupling reactions. *Inorg. Chim. Acta* **2015**, *427*, 226–231. [CrossRef]
19. Gong, Y.-Q.; Fan, J.; Wang, R.-H.; Zhou, Y.-F.; Yuan, D.-Q.; Hong, M.-C. Syntheses, crystal structures and photoluminescence of two Cd(II) coordination polymers derived from a flexible bipyridyl ligand. *J. Mol. Struct.* **2004**, *705*, 29–34. [CrossRef]

20. Li, W.; Evans, O.-R.; Xiong, R.-G.; Wang, Z. Supramolecular Engineering of Chiral and Acentric 2D Networks. Synthesis, Structures, and Second-Order Nonlinear Optical Properties of Bis(nicotinato)zinc and Bis{3-[2-(4-pyridyl)ethenyl]benzoato}cadmium. *J. Am. Chem. Soc.* **1998**, *120*, 13272–13273.
21. Lin, W.; Wang, Z.; Ma, L. A Novel Octupolar Metal−Organic NLO Material Based on a Chiral 2D Coordination Network. *J. Am. Chem. Soc.* **1999**, *121*, 11249–11250. [CrossRef]
22. Chen, Y.-B.; Zhang, J.; Cheng, J.-K.; Kang, Y.; Li, Z.-J.; Yao, Y.-G. 1D chain structure, NLO and luminescence properties of [Zn_2 (bpp) $(pht)_2$]. *Inorg. Chem. Commun.* **2004**, *7*, 1139–1141. [CrossRef]
23. Cooke, N.H.C.; Viavattene, R.L.; Eksteen, R.; Wong, W.S.; Davies, G.; Karger, B.L. Use of metal ions for selective separations in high-performance liquid chromatography. *J. Chromatogr.* **1978**, *149*, 391–415. [CrossRef]
24. Le Page, J.N.; Lindner, W.; Davies, G.; Seitz, D.E.; Karger, B.L. Resolution of the optical isomers of dansyl amino acids by reversed phase liquid chromatography with optically active metal chelate additives. *Anal. Chem.* **1979**, *51*, 433–435. [CrossRef]
25. Lindner, W. HPLC-Enantiomerentrennung an gebundenen chiralen Phasen. *Naturwissenschaften* **1980**, *67*, 354–356. [CrossRef]
26. Hashemi, L.; Hosseinifard, M.; Amani, V.; Morsali, A.J. Sonochemical Synthesis of Two New Nano-structured Cadmium (II) Supramolecular Complexes. *Inorg. Organomet. Polym.* **2013**, *23*, 519–524. [CrossRef]
27. Mlowe, S.; Lewis, D.J.; Malik, M.A.; Raftery, J.; Mubofu, E.B.; O'Brien, P.; Revaprasadu, N. Bis(piperidinedithiocarbamato)pyridine cadmium(II) as a single-source precursor for the synthesis of CdS nanoparticles and aerosol-assisted chemical vapour deposition (AACVD) of CdS thin films. *New J. Chem.* **2014**, *38*, 6073–6080. [CrossRef]
28. Stang, P.J.; Olenyuk, B. Self-Assembly, Symmetry, and Molecular Architecture: Coordination as the Motif in the Rational Design of Supramolecular Metallacyclic Polygons and Polyhedra. *Acc. Chem. Res.* **1997**, *30*, 502–518. [CrossRef]
29. Braga, D.; Grepioni, F.; Desiraju, G.R. Crystal Engineering and Organometallic Architecture. *Chem. Rev.* **1998**, *98*, 1375–1406. [CrossRef]
30. Yaghi, O.M.; Li, H.; Davis, C.; Richardson, D.; Groy, T.L. Synthetic Strategies, Structure Patterns, and Emerging Properties in the Chemistry of Modular Porous Solids. *Acc. Chem. Res.* **1998**, *31*, 474–484. [CrossRef]
31. Purdy, A.P.; Gilardi, R.; Luther, J.; Butcher, R.J. Synthesis, crystal structure, and reactivity of alkali and silver salts of sulfonated imidazoles. *Polyhedron* **2007**, *26*, 3930–3938. [CrossRef]
32. Zhang, Z.-T.; Shi, J.; He, Y.; Guo, Y.-N. Self-assembly and crystal structure of a barium sulfonate chrysin coordination polymer. *Inorg. Chem. Commun.* **2006**, *9*, 579–581. [CrossRef]
33. Yang, X.-L.; Ren, S.-B.; Zhang, J.; Li, Y.-Z.; Du, H.-B.; You, X.-Z. Syntheses and structures of three coordination polymers based on 4-methylbenzenethiolates of Zn(II) and Cd(II) and bipyridine. *J. Coord. Chem.* **2009**, *62*, 3782–3794. [CrossRef]
34. Ghoshal, D.; Maji, T.K.; Mostafa, G.; Lu, T.H.; Chaudhuri, N.R. A Three-dimensional honeycomb-Like network constructed with novel "Sinusoidal" One-Dimensional Chains via Hydrogen Bonding and π−π Interactions. *Cryst. Growth Des.* **2003**, *3*, 9–11. [CrossRef]
35. Rashidi-Ranjbar, Z.; Hamidi, S.; Heshmatpour, F.; Morsali, A. Thermal, spectroscopic, X-ray powder diffraction, and structural studies on a new Cd(II) mixed-ligand coordination polymer. *J. Coord. Chem.* **2009**, *62*, 2022–2027. [CrossRef]
36. Smith, G.; Wermuth, U.D.; Young, D.J.; White, J.M. Polymeric structures in the metal complexes of 5-sulfosalicylic acid: The rubidium(I), caesium(I) and lead(II) analogues. *Polyhedron* **2007**, *26*, 3645–3652. [CrossRef]
37. Wang, C.-J.; Ren, P.-D.; Zhang, Z.-B.; Fang, Y.; Wang, Y.-Y. Synthesis and characterization of a nickel-organic framework encapsulating hetero-chiral helical water chains in the 1-D channels. *J. Coord. Chem.* **2009**, *62*, 2814–2823. [CrossRef]
38. De Silva, C.-R.; Maeyer, J.-R.; Dawson, A.; Zheng, Z. Adducts of lanthanide β-diketonates with 2,4,6-tri(2-pyridyl)-1,3,5-triazine: Synthesis, structural characterization, and photoluminescence studies. *Polyhedron* **2007**, *26*, 1229–1238. [CrossRef]
39. Ionova, G.; Raber, C.; Guillaumont, R.; Ionov, S.; Madic, C.; Krupa, D.; Guillaneux, J.-C. A donor–acceptor model of Ln(III) complexation with terdentate nitrogen planar ligands. *New J. Chem.* **2002**, *26*, 234–242. [CrossRef]
40. Yan, C.; Chen, Q.; Chen, L.; Feng, R.; Shan, X.; Jiang, F.; Hong, M. crystal structures and luminescence behaviour of d^{10} Metal–Organic Complexes with multipyridineligands. *Aust. J. Chem.* **2011**, *64*, 104–118. [CrossRef]
41. Wu, G.; Wang, X.-F.; Guo, L.; Li, H.-H. Zn(II) and Cd(II) Complexes extended structures sustained by hydrogen bonding, π–π and C–H···π interactions. *J. Chem. Crystallogr.* **2011**, *41*, 1071–1076. [CrossRef]
42. Glaser, T.; Lügger, T.; Fröhlich, R. Synthesis, crystal structures, and magnetic properties of a mono- and a dinuclearcopper(II) complex of the 2,4,6-tris(2-pyridyl)-1,3,5-triazine ligand. *Eur. J. Inorg. Chem.* **2004**, 394–400. [CrossRef]
43. Schwalbe, M.; Karnahl, M.; Görls, H.; Chartrand, D.; Laverdiere, F.; Hanan, G.-S.; Tschierlei, S.; Dietzek, B.; Schmitt, M.; Popp, J.; et al. Ruthenium polypyridine complexes of tris-(2-pyridyl)-1,3,5-triazine—Unusual building blocks for the synthesis of photochemical molecular devices. *Dalton Trans.* **2009**, 4012–4022. [CrossRef] [PubMed]
44. Soliman, S.M.; El-Faham, A. Synthesis, characterization, and structural studies of two heteroleptic Mn(II) complexes with tridentate N,N,N-pincer type ligand. *J. Coord. Chem.* **2018**, *71*, 2373–2388. [CrossRef]
45. Soliman, S.M.; El-Faham, A. One pot synthesis of two Mn(II) perchlorate complexes with s-triazine *NNN*-pincer ligand; molecular structure, Hirshfeld analysis and DFT studies. *J. Mol. Struct.* **2018**, *1164*, 344–353. [CrossRef]
46. Soliman, S.M.; El-Faham, A.; Elsilk, S.E.; Farooq, M. Two heptacoordinatedmanganese(II) complexes of giant pentadentate s-triazine bis-Schiff base ligand: Synthesis, crystal structure, biological and DFT studies. *Inorg. Chim. Acta* **2018**, *479*, 275–285. [CrossRef]

47. Moulton, C.J.; Shaw, B.L. Transition metal–carbon bonds. Part XLII. Complexes of nickel, palladium, platinum, rhodium and iridium with the tridentate ligand 2,6-bis[(di-t-butylphosphino)methyl]phenyl. *J. Chem. Soc. Dalton Trans.* **1976**, 1020–1040. [CrossRef]
48. Van Koten, G. Tuning the reactivity of metals held in a rigid ligand environment. *Pure Appl. Chem.* **1989**, *61*, 1681–1694. [CrossRef]
49. Albrecht, M.; Van Koten, G. Platinum Group Organometallics Based on "Pincer" Complexes: Sensors, Switches, and Catalysts. *Angew. Chem. Int. Ed. Engl.* **2001**, *40*, 3750–3781. [CrossRef]
50. Asay, M.; Morales-Morales, D. Non-symmetric pincer ligands: Complexes and applications in catalysis. *J. Chem. Soc. Dalton Trans.* **2015**, *44*, 17432–17447. [CrossRef]
51. Li, H.; Zheng, B.; Huang, K.-W. A new class of PN_3-pincer ligands for metal–ligand cooperative catalysis. *Coord. Chem. Rev.* **2015**, *293*, 116–138. [CrossRef]
52. Szabó, K.J. Mechanism of the oxidative addition of hypervalent iodonium salts to palladium(II) pincer-complexes. *J. Mol. Catal. A Chem.* **2010**, *324*, 56–63. [CrossRef]
53. De Hoog, P.; Gamez, P.; Driessen, L.W.; Reedijk, J. New polydentate and polynucleating *N*-donor ligands from amines and 2,4,6-trichloro-1,3,5-triazine. *Tetrahedron Lett.* **2002**, *43*, 6783–6786. [CrossRef]
54. Das, A.; Demeshko, S.; Dechert, S.; Meyer, F. A New Triazine-Based Tricompartmental Ligand for Stepwise Assembly of Mononuclear, Dinuclear, and 1D-Polymeric Heptacoordinate Manganese(II)/Azido Complexes. *Eur. J. Inorg. Chem.* **2011**, *2011*, 1240–1248. [CrossRef]
55. Medlycott, E.A.; Udachin, K.A.; Hanan, G.S. Non-covalent polymerisation in the solid state: Halogen–halogen *vs*. methyl–methyl interactions in the complexes of 2,4-di(2-pyridyl)-1,3,5-triazine ligands. *Dalton Trans.* **2007**, 430–438. [CrossRef] [PubMed]
56. Mooibroek, T.J.; Gamez, P. The s-triazine ring, a remarkable unit to generate supramolecular interactions. *Inorg. Chim. Acta* **2007**, *360*, 381–404. [CrossRef]
57. Gamez, P.; Reedijk, J. 1,3,5-Triazine-Based Synthons in Supramolecular Chemistry. *Eur. J. Inorg. Chem.* **2006**, *2006*, 29–42. [CrossRef]
58. Ranganathan, A.; Heisen, B.C.; Dix, I.; Meyer, F. A triazine-based three-directional rigid-rod tecton forms a novel 1D channel structure. *Chem. Commun.* **2007**, 3637–3639. [CrossRef]
59. Galan-Mascaros, J.R.; Clemente-Juan, J.M.; Dunbar, K.R. Synthesis, structure and magnetic properties of the one-dimensional chain compound $\{K[Fe(1,3,5\text{-triazine-2,4,6-tricarboxylate})(H_2O)_2]\cdot 2H_2O\}_\infty$. *J. Chem. Soc. Dalton Trans.* **2002**, 2710–2713. [CrossRef]
60. Wietzke, R.; Mazzanti, M.; Latour, J.M.; Percaut, J. Crystal Structure and Solution Fluxionality of Lanthanide Complexes of 2,4,6,-Tris-2-pyridyl-1,3,5-triazine. *Inorg. Chem.* **1999**, *38*, 3581–3585. [CrossRef]
61. Ramirez, J.; Stadler, A.-M.; Kyritskas, N.; Lehn, J.-M. Solvent-modulated reversible conversion of a [2 × 2]-grid into a pincer-like complex. *Chem. Commun.* **2007**, 237–239. [CrossRef] [PubMed]
62. Ramírez, J.; Stadler, A.M.; Harrowfield, J.M.; Brelot, L.; Huuskonen, J.; Rissanen, K.; Allouche, L.; Lehn, J.M. Coordination Architectures of Large Heavy Metal Cations (Hg^{2+} and Pb^{2+}) with Bis-tridentate Ligands: Solution and Solid-State Studies. *Z. Anorg. Allg. Chem.* **2007**, *633*, 2435–2444. [CrossRef]
63. Ramirez, J.; Stadler, A.-M.; Brelot, L.; Lehn, J.-M. Coordinative, conformational and motional behaviour of triazine-based ligand strands on binding of Pb(II) cations. *Tetrahedron* **2008**, *64*, 8402–8410. [CrossRef]
64. Hsu, G.-Y.; Misra, P.; Cheng, S.-C.; Wei, H.-H.; Mohanta, S. Syntheses, structures, and magnetic properties of dicyanamide bridged one-dimensional double chain and discrete dinuclear complexes of manganese(II) derived from 6,7-dimethyl-2,3-di(2-pyridyl)quinoxaline or 2,4,6-tri(2-pyridyl)-1,3,5-triazine. *Polyhedron* **2006**, *25*, 3393–3398. [CrossRef]
65. Zhang, M.; Fang, R.; Zhao, Q. Synthesis and Crystal Structure of $[Mn(H_2O)(tptz)(CH_3COO)][N(CN)_2] \cdot 2H_2O$ (tptz = 2,4,6-tris-(2-pyridyl)-1,3,5-triazine). *J. Chem. Crystallogr.* **2008**, *38*, 601–604. [CrossRef]
66. Tyagi, P.; Singh, U.P. Chloro and azido bonded manganese complexes: Synthesis, structural, and magnetic studies. *J. Coord. Chem.* **2009**, *62*, 1613–1622. [CrossRef]
67. Soliman, S.M.; Almarhoon, Z.; El-Faham, A. Synthesis, Molecular and Supramolecular Structures of New Cd(II) Pincer-Type Complexes with *s*-Triazine Core Ligand. *Crystals* **2019**, *9*, 226. [CrossRef]
68. Soliman, S.M.; Elsilk, S.E.; El-Faham, A. Syntheses, structure, Hirshfeld analysis and antimicrobial activity of four new Co(II) complexes with *s*-triazine-based pincer ligand. *Inorg. Chim. Acta* **2020**, *510*, 119753. [CrossRef]
69. Soliman, S.M.; El-Faham, A. Synthesis, molecular structure and DFT studies of two heteroleptic nickel(II) s-triazine pincer type complexes. *J. Mol. Struct.* **2019**, *1185*, 461–468. [CrossRef]
70. Soliman, S.M.; Elsilk, S.E.; El-Faham, A. Synthesis, structure and biological activity of zinc(II) pincer complexes with 2,4-*bis*(3,5-dimethyl-1*H*-pyrazol-1-yl)-6-methoxy-1,3,5-triazine. *Inorg. Chim. Acta* **2020**, *508*, 119627. [CrossRef]
71. Soliman, S.M.; El-Faham, A. Synthesis, X-ray structure, and DFT studies of five- and eight-coordinated Cd(II) complexes with s-triazine N-pincer chelate. *J. Coord. Chem.* **2019**, *73*, 1621–1636. [CrossRef]
72. Barakat, A.; El-Faham, A.; Haukka, M.; Al-Majid, A.M.; Soliman, S.M. s-Triazine Pincer Ligands: Synthesis of their Metal Complexes, Coordination Behavior, and Applications. *App. Organomet. Chem.* **2021**, *35*, e6317. [CrossRef]
73. Soliman, S.M.; Almarhoon, Z.; Sholkamy, E.N.; El-Faham, A. *Bis*-pyrazolyl-*s*-triazine Ni(II) pincer complexes as selective gram positive antibacterial agents; synthesis, structural and antimicrobial studies. *J. Mol. Struct.* **2019**, *1195*, 315–322. [CrossRef]
74. Wang, X.; Xing, Y.H.; Bai, F.Y.; Wang, X.Y.; Guan, Q.L.; Hou, Y.N.; Zhang, R.; Shi, Z. Synthesis, structure, and surface photovoltage properties of a series of novel d^7–d^{10} metal complexes with pincer N-heterocycle ligands. *RSC Adv.* **2013**, *3*, 16021. [CrossRef]

75. Sheldrick, G.M. A short history of SHELX. *Acta Cryst. A* **2008**, *64*, 112–122. [CrossRef] [PubMed]
76. Spackman, M.A.; Jayatilaka, D. Hirshfeld Surface Analysis. *CrystEngComm* **2009**, *11*, 19–32. [CrossRef]
77. Jelsch, C.; Ejsmont, K.; Hudera, L. The enrichment ratio of atomic contacts in crystals, an indicator derived from the Hirshfeld surface analysis. *IUCrJ* **2014**, *1*, 119–128. [CrossRef]

Disclaimer/Publisher's Note: The statements, opinions and data contained in all publications are solely those of the individual author(s) and contributor(s) and not of MDPI and/or the editor(s). MDPI and/or the editor(s) disclaim responsibility for any injury to people or property resulting from any ideas, methods, instructions or products referred to in the content.